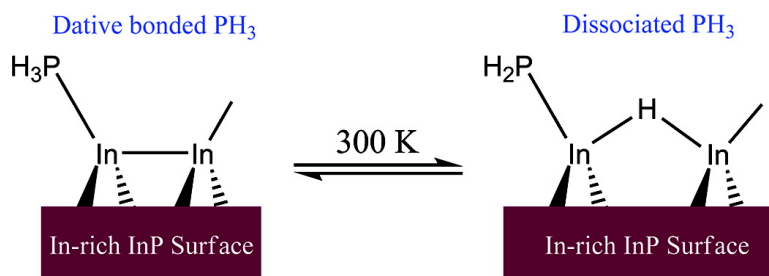


## Phosphine Adsorption on the In-Rich InP(001) Surface: Evidence of Surface Dative Bonds at Room Temperature

Ujjal Das, and Krishnan Raghavachari Robyn L. Woo, and Robert F. Hicks

*Langmuir*, 2007, 23 (20), 10109-10115 • DOI: 10.1021/la700790h

Downloaded from <http://pubs.acs.org> on November 25, 2008



### More About This Article

Additional resources and features associated with this article are available within the HTML version:

- Supporting Information
- Links to the 1 articles that cite this article, as of the time of this article download
- Access to high resolution figures
- Links to articles and content related to this article
- Copyright permission to reproduce figures and/or text from this article

[View the Full Text HTML](#)



# Phosphine Adsorption on the In-Rich InP(001) Surface: Evidence of Surface Dative Bonds at Room Temperature

Ujjal Das and Krishnan Raghavachari\*

*Department of Chemistry, Indiana University, Bloomington, Indiana 47405*

Robyn L. Woo and Robert F. Hicks\*

*Department of Chemical and Biomolecular Engineering, University of California, Los Angeles, California 90095*

*Received March 16, 2007. In Final Form: July 6, 2007*

Adsorption of phosphine on indium phosphide compound semiconductor surfaces is a key process during the chemical vapor deposition of this material. Recent experimental infrared studies of the In-rich InP surfaces exposed to phosphine show a complex vibrational pattern in the P–H stretch region, presumably due to overlapping contributions from several structural species. We have performed density functional calculations using finite-sized cluster models to investigate the dissociative adsorption of PH<sub>3</sub> on the In-rich InP surface. We find that initially PH<sub>3</sub> forms a dative bond with one of the surface In atoms with a binding energy of approximately 11 kcal mol<sup>-1</sup> at 298 K. The In–PH<sub>3</sub> bond length is 2.9 Å, 0.3 Å greater than the In–P covalent bond length computed for In–PH<sub>2</sub> species produced by hydrogen migration to a neighboring atom. However, the dissociation process, though exothermic, involves a significant activation barrier of ~23 kcal mol<sup>-1</sup>, suggesting the possibility of metastable trapping of the dative bonded PH<sub>3</sub> molecules. Indeed, a careful vibrational analysis of different P–H stretching modes of the surface-bound PH<sub>3</sub> and PH<sub>2</sub> units gives excellent agreement with the observed infrared frequencies and their relative intensities. Moreover, at higher temperatures the frequency modes associated with PH<sub>3</sub> disappear either due to desorption or dissociation of this molecule, an observation also well supported from the computed thermochemical parameters at different temperatures. The computed energy parameters and infrared analysis provide direct evidence that PH<sub>3</sub> is present as a dative bonded complex on the InP surface at room temperature.

## 1. Introduction

Chemisorption of molecules on a semiconductor surface is a key process that can passivate the surface and alter its electronic and optical properties. In many cases, the initial adsorption is governed by the formation of a dative bonded complex between an electron-rich center in the substrate molecule and an empty surface dangling bond.<sup>1–4</sup> However, such dative bonded complexes are, in general, metastable and, therefore, either desorb from the surface or dissociate into a thermodynamically more favorable state. As a consequence, the examples of molecularly adsorbed species on semiconductor surfaces observed at room temperature are limited, especially when the substrate molecule is a simple hydride.

Bozso et al. showed that ammonia dissociates on the Si(100)-2 × 1 surface at a temperature as low as 90 K.<sup>5</sup> Phosphine adsorption on Si(100) surface has also been extensively studied and, like ammonia, is known to chemisorb molecularly followed by rapid dissociation into PH<sub>2</sub> and H at 200 K.<sup>6</sup> The stability of the dissociated species at room temperature has been recently confirmed by Schofield and co-workers using atomically resolved STM images.<sup>7,8</sup> In comparison, adsorption of arsine on silicon surfaces has received relatively minor attention. The lone

experiment by Kipp et al.<sup>9</sup> and a couple of theoretical works<sup>10,11</sup> suggest a possible dissociation of AsH<sub>3</sub> at room temperature. In the case of primary and secondary amines, the initial dative bonded complex undergoes N–H dissociation at 300 K.<sup>3</sup> Tertiary amines, which lack an N–H bond, do not dissociate and instead remain bound to the surface in a dative bonded state.<sup>4</sup>

On the Ge(100)-2 × 1 surface, NH<sub>3</sub> adsorbs molecularly, and this form is stable between 130 and 200 K, after which it desorbs preferentially because of its low binding energy relative to the dissociation energy barrier as shown in a recent cluster calculation by Mui et al.<sup>12</sup> Barring a single theoretical calculation,<sup>13</sup> very little is known about PH<sub>3</sub> and AsH<sub>3</sub> adsorption on Ge. However, unlike Si, all substituted amines are stable as dative-bonded complexes on Ge surfaces. This stability is attributed to the high binding energy of the amine molecules and low proton affinity of the surface. In particular, Bent and co-workers computed this binding energy to be approximately 25 kcal/mol using density functional theory.<sup>14</sup>

\* Authors to whom correspondence may be directed. E-mail: kraghava@indiana.edu; rhicks@ucla.edu.

(1) Loscutoff, P. W.; Bent, S. F. *Annu. Rev. Phys. Chem.* **2006**, *57*, 467.  
 (2) Filler, M. A.; Van Deventer, J. A.; Keung, A. J.; Bent, S. F. *J. Am. Chem. Soc.* **2006**, *128*, 770.  
 (3) Mui, C.; Wang, G. T.; Bent, S. F.; Musgrave, C. B. *J. Chem. Phys.* **2001**, *114*, 10170.  
 (4) Cao, X. P.; Hamers, R. J. *J. Am. Chem. Soc.* **2001**, *123*, 10988.  
 (5) Bozso, F.; Avouris, P. *Phys. Rev. Lett.* **1986**, *57*, 1185.  
 (6) Shan, J.; Wang, Y. J.; Hamers, R. J. *J. Phys. Chem.* **1996**, *100*, 4961.

(7) Schofield, S. R.; Curson, N. J.; Warschkow, O.; Marks, N. A.; Wilson, H. F.; Simmons, M. Y.; Smith, P. V.; Radny, M. W.; McKenzie, D. R.; Clark, R. G. *J. Phys. Chem. B* **2006**, *110*, 3173.

(8) Wilson, H. F.; Warschkow, O.; Marks, N. A.; Schofield, S. R.; Curson, N. J.; Smith, P. V.; Radny, M. W.; McKenzie, D. R.; Simmons, M. Y. *Phys. Rev. Lett.* **2004**, *93*, 226102.

(9) Kipp, L.; Bringans, R. D.; Biegelsen, D. K.; Swartz, L. E.; Hicks, R. F. *Phys. Rev. B* **1994**, *50*, 5448.

(10) McDonnell, T. L.; Marks, N. A.; Warschkow, O.; Wilson, H. F.; Smith, P. V.; Radny, M. W. *Phys. Rev. B* **2005**, *72*, 193307.

(11) Miotto, R.; Srivastava, G. P.; Miwa, R. H.; Ferraz, A. C. *J. Chem. Phys.* **2001**, *114*, 9549.

(12) Mui, C.; Musgrave, C. B. *Langmuir* **2005**, *21*, 5230.

(13) Miotto, R.; Ferraz, A. C.; Srivastava, G. P. *Braz. J. Phys.* **2002**, *32*, 392.

(14) Mui, C.; Han, J. H.; Wang, G. T.; Musgrave, C. B.; Bent, S. F. *J. Am. Chem. Soc.* **2002**, *124*, 4027.

In contrast, the detailed mechanism of molecular adsorption and subsequent dissociation on compound semiconductor surfaces such as gallium arsenide (GaAs) and indium phosphide (InP) has received relatively minor attention. The experimental study by Apen et al. suggests that a recombinative desorption of ( $\text{NH}_2 + \text{H}$ ) is the dominant reaction channel for ammonia on GaAs-(100) at temperatures above 250 K.<sup>15</sup> Presence of both  $\text{PH}_3$  and  $\text{PH}_2$  on this surface following  $\text{PH}_3$  adsorption at 140 K has also been reported.<sup>16,17</sup> For  $\text{AsH}_3$ , White and co-workers observed that dissociative adsorption is the primary reaction channel starting from 140 K.<sup>18,19</sup> However, in a recent infrared study combined with ab initio cluster calculations, Fu et al. found that dative bonded arsine is present on GaAs surface even at 300 K.<sup>20</sup> As for InP, except in a few kinetic studies,<sup>21,22</sup> adsorption of hydride precursors on this surface has not been the focus of detailed investigations.<sup>23,24</sup>

It is thus clear that molecularly adsorbed states on semiconductor surfaces are, in general, transient intermediates for group V hydrides and, therefore, are not observed at room temperature. They are only stabilized when one or more hydrogens is substituted and the resulting complexes have relatively high binding energy. In this paper, we investigate the adsorption of  $\text{PH}_3$  on the In-rich InP(100)- $\delta(2 \times 4)$  surface using ab initio quantum chemical cluster calculations. This work combined with our recently reported surface infrared spectra<sup>25</sup> provides definitive information about significant trapping of the initial dative bonded complex at room temperature. The binding energy of phosphine in this complex is relatively low ( $\sim 11$  kcal/mol), which supports the known poor sticking probability of the molecule.<sup>21</sup> In addition, this weakly bound complex is only a metastable state since dissociation of phosphine results in a more stable surface species. Despite all these facts, the dative bonded state is prevalent in equilibrium at room temperature, presumably due to high kinetic barrier for  $\text{PH}_3$  dissociation coupled with the relatively low thermodynamic stability of the dissociated products.

## 2. Computational Details

The In-rich surface of InP exhibits relatively complex surface reconstructions. For example, the  $\delta(2 \times 4)$  surface considered in this study has one In–P adatom dimer on top of four surface In–In dimers in each unit cell.<sup>26</sup> A cluster model has been designed accordingly that represents such a surface structure. This is shown in Figure 1. This model is sufficiently large and retains all the salient features of the reconstructed surface.<sup>27,28</sup> In III–V compound semiconductors, each one of the bulk III and V atoms are four-fold coordinated, sharing three covalent and one dative bond between them. To achieve a proper balance between covalent and dative

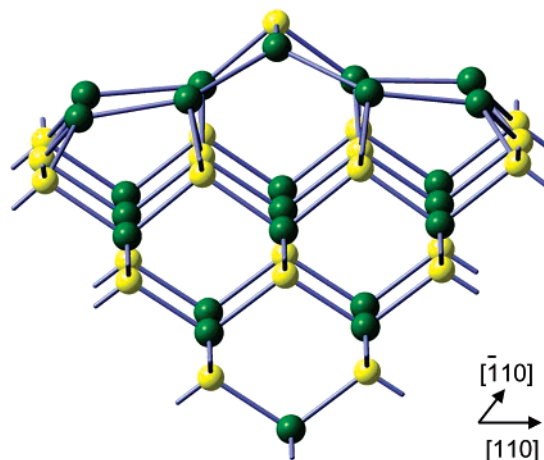


**Figure 1.** An optimized cluster model for the In-rich InP surface. Note that the four In–In dimers are parallel to the [110] axis and perpendicular to the direction of the In–P mixed dimer. Color code: green (In) and yellow (P).

bonding in our cluster model, two of the second-layer phosphorus atoms are terminated with lone pairs, while the remainder of the bulk In and P atoms are truncated with hydrogens. We used the standard B3LYP hybrid density functional available in the Gaussian 03 quantum chemistry suite for optimization and vibrational analysis.<sup>29–31</sup> We employed the all-electron (18s/14p/9d)/[6s/5p/3d] contracted basis set for the surface indium atoms, the Dunning–Huzinaga (11s/7p/1d)/[6s/4p/1d] contracted basis set (D95\*\*) for phosphorus, the D95\*\* polarized double- $\zeta$  basis set for the surface hydrogen atoms, and the D95 double- $\zeta$  basis set for the terminating hydrogen atoms.<sup>32–34</sup> The remaining indium atoms were treated using the pseudopotential-based SDD basis set to make the computations feasible.<sup>35</sup> In sum, the different basis sets used in this study have been denoted as “GEN” basis. Starting from the third layer, all the In and P atoms, along with their attached H atoms, were frozen along tetrahedral directions (In–P = 2.54 Å, In–H = 1.76 Å, P–H = 1.42 Å), while the remaining atoms (in the top two layers, the adatoms, and the adsorbate atoms) were fully allowed to relax. We noticed in an earlier study that the neglect of anharmonicity in the vibrational analysis (along with other deficiencies in our theoretical models) leads to a systematic overestimation of the computed P–H stretching frequencies by approximately  $110 \text{ cm}^{-1}$ .<sup>36</sup> We have, therefore, uniformly shifted down all the calculated frequencies by this correction factor to compare them with the experiment.

(15) Apen, E.; Gland, J. L. *Surf. Sci.* **1994**, *321*, 301.  
 (16) Sun, Y. M.; Huett, T.; Sloan, D.; White, J. M. *J. Vac. Sci. Technol., A* **1994**, *12*, 2287.  
 (17) Singh, N. K.; Murrell, A. J.; Foord, J. S. *Surf. Sci.* **1992**, *274*, 341.  
 (18) Zhu, X. Y.; Wolf, M.; Huett, T.; Nail, J.; Banse, B. A.; Creighton, J. R.; White, J. M. *Appl. Phys. Lett.* **1992**, *60*, 977.  
 (19) Wolf, M.; Zhu, X. Y.; Huett, T.; White, J. M. *Surf. Sci.* **1992**, *275*, 41.  
 (20) Fu, Q.; Li, L.; Li, C. H.; Begarney, M. J.; Law, D. C.; Hicks, R. F. *J. Phys. Chem. B* **2000**, *104*, 5595.  
 (21) Sun, Y.; Law, D. C.; Hicks, R. F. *Surf. Sci.* **2003**, *540*, 12.  
 (22) Sun, Y.; Law, D. C.; Visbeck, S. B.; Hicks, R. F. *Surf. Sci.* **2002**, *513*, 256.  
 (23) Henrion, O.; Klein, A.; Jaegermann, W. *Surf. Sci.* **2000**, *457*, L337.  
 (24) Hung, W. H.; Chen, H. C.; Chang, C. C.; Hsieh, J. T.; Hwang, H. L. *J. Phys. Chem. B* **1999**, *103*, 3663.  
 (25) Woo, R. L.; Das, U.; Cheng, S. F.; Chen, G.; Raghavachari, K.; Hicks, R. F. *Surf. Sci.* **2006**, *600*, 4888.  
 (26) Li, L.; Fu, Q.; Li, C. H.; Han, B. K.; Hicks, R. F. *Phys. Rev. B* **2000**, *61*, 10223.  
 (27) Mirbt, S.; Moll, N.; Cho, K.; Joannopoulos, J. D. *Phys. Rev. B* **1999**, *60*, 13283.  
 (28) Schmidt, W. G.; Bechstedt, F.; Esser, N.; Pristovsek, M.; Schultz, C.; Richter, W. *Phys. Rev. B* **1998**, *57*, 14596.

(29) Frisch, M. J.; Trucks, G. W.; Schlegel, H. B.; Scuseria, G. E.; Robb, M. A.; Cheeseman, J. R.; Montgomery, J. A., Jr.; Vreven, T.; Kudin, K. N.; Burant, J. C.; Millam, J. M.; Iyengar, S. S.; Tomasi, J.; Barone, V.; Mennucci, B.; Cossi, M.; Scalmani, G.; Rega, N.; Petersson, G. A.; Nakatsuji, H.; Hada, M.; Ehara, M.; Toyota, K.; Fukuda, R.; Hasegawa, J.; Ishida, M.; Nakajima, T.; Honda, Y.; Kitao, O.; Nakai, H.; Klene, M.; Li, X.; Knox, J. E.; Hratchian, H. P.; Cross, J. B.; Bakken, V.; Adamo, C.; Jaramillo, J.; Gomperts, R.; Stratmann, R. E.; Yazyev, O.; Austin, A. J.; Cammi, R.; Pomelli, C.; Ochterski, J. W.; Ayala, P. Y.; Morokuma, K.; Voth, G. A.; Salvador, P.; Dannenberg, J. J.; Zakrzewski, V. G.; Dapprich, S.; Daniels, A. D.; Strain, M. C.; Farkas, O.; Malick, D. K.; Rabuck, A. D.; Raghavachari, K.; Foresman, J. B.; Ortiz, J. V.; Cui, Q.; Baboul, A. G.; Clifford, S.; Cioslowski, J.; Stefanov, B. B.; Liu, G.; Liashenko, A.; Piskorz, P.; Komaromi, I.; Martin, R. L.; Fox, D. J.; Keith, T.; Al-Laham, M. A.; Peng, C. Y.; Nanayakkara, A.; Challacombe, M.; Gill, P. M. W.; Johnson, B.; Chen, W.; Wong, M. W.; Gonzalez, C.; Pople, J. A. *Gaussian 03*; Gaussian, Inc.: Wallingford, CT, 2004.  
 (30) Becke, A. D. *J. Chem. Phys.* **1993**, *98*, 1372.  
 (31) Lee, C. T.; Yang, W. T.; Parr, R. G. *Phys. Rev. B* **1988**, *37*, 785.  
 (32) Bergner, A.; Dolg, M.; Kuchle, W.; Stoll, H.; Preuss, H. *Mol. Phys.* **1993**, *80*, 1431.  
 (33) Godbout, N.; Salahub, D. R.; Andzelm, J.; Wimmer, E. *Can. J. Chem. - Rev. Can. Chim.* **1992**, *70*, 560.  
 (34) Dunning, T. H. J.; Hay, P. J. In *Methods in Electronic Structure Theory*; Schaefer, H. F., III, Ed.; Modern Theoretical Chemistry, Vol. 3; Plenum: New York, 1976.  
 (35) Igelmann, G.; Stoll, H.; Preuss, H. *Mol. Phys.* **1988**, *65*, 1321.  
 (36) Fu, Q.; Negro, E.; Chen, G.; Law, D. C.; Li, C. H.; Hicks, R. F.; Raghavachari, K. *Phys. Rev. B* **2002**, *65*.

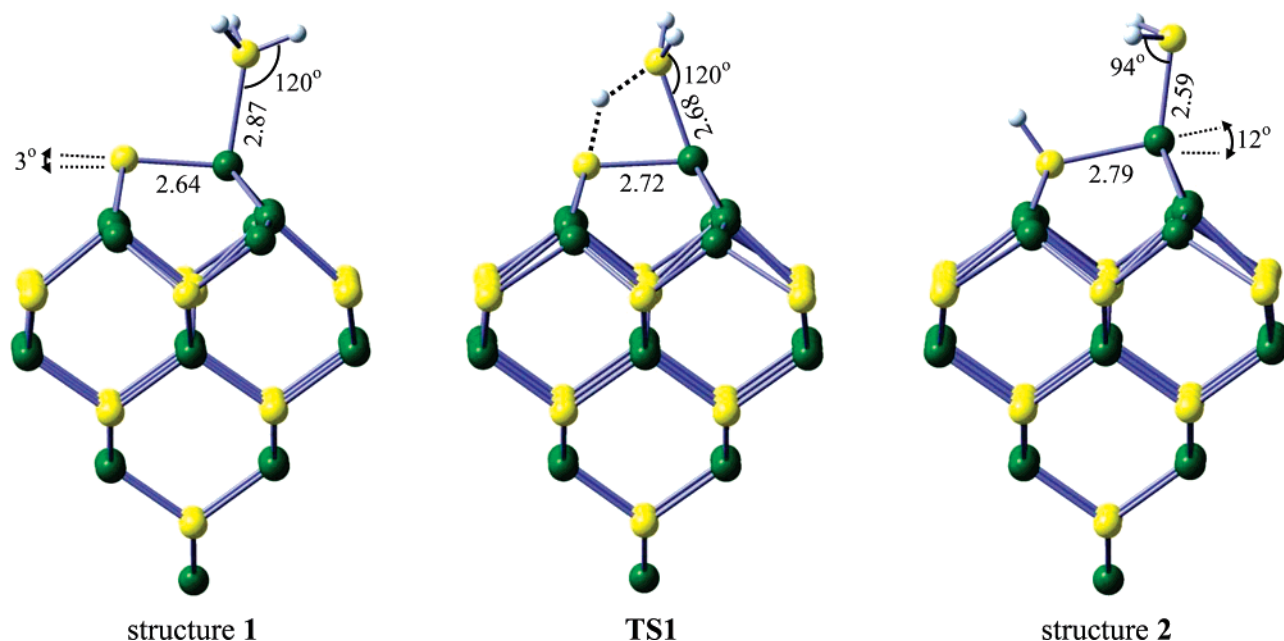


**Figure 2.** Surface structures after phosphine adsorption on the In–P mixed dimer. The dative bonded complex (**1**, left), transition state for dissociation (**TS1**, middle), and the dissociated species (**2**, right) are shown here. The distances are in Å.

Shown later in Figure 6a are the infrared spectra of the phosphine-adsorbed indium phosphide  $\delta(2 \times 4)$  surface at room temperature. In particular, spectra recorded using two different polarizations (*s* and *p*) for light propagation along the [110] direction are shown. In the inset of Figure 6a, the deconvoluted bands in the P–H stretch region, the focus of this study, are also shown. This part of the spectrum shows a complex pattern containing nine overlapping bands within  $150 \text{ cm}^{-1}$ . The experimental set up for recording these spectra can be found in reference 25.

### 3. Results and Discussion

**3.1. Surface Structure.** *3.1.1. PH<sub>3</sub> Adsorption on the In–P Mixed Dimer.* The  $\delta(2 \times 4)$  surface has two different binding sites, the In–P mixed dimer and the In–In dimers. We begin our discussion considering PH<sub>3</sub> adsorption on the In–P mixed dimer. Presence of a lone pair on the P atom introduces an uneven charge distribution within this dimer. This results in an electron-rich, nucleophilic “up” atom (in this case P) and an electron-deficient, electrophilic “down” atom. Similar dimer buckling and zwitterionic character were also observed on Si and Ge surfaces.<sup>14</sup> Structure **1** in Figure 2 presents a dative-bonded In–PH<sub>3</sub> species resulting from interaction of PH<sub>3</sub> lone pair with the down-buckled In atom. The dative bond formation is exothermic with respect to the entrance level (bare surface + gas-phase phosphine). This is illustrated in the potential energy diagram presented in Figure 3. We compute the binding energy to be 8.5 kcal/mol at the B3LYP/GEN level. For comparison, Fu et al. reported the binding energy of arsine on GaAs surface to be 9.3 kcal/mol.<sup>20</sup>

Note that though density functional theory is effective in modeling strong interactions such as covalent bonding, it may not adequately describe the weaker interactions in dative bonded complexes where van der Waals or dispersion forces may play a role. For this reason, the accuracy of the binding energy calculation was further assessed by considering H<sub>3</sub>In–PH<sub>3</sub> as a model system. Applying the same model chemistry used in this work (B3LYP/GEN), phosphine binding energy in H<sub>3</sub>In–PH<sub>3</sub> was found to be 10.0 kcal/mol. However, CCSD(T) single-point calculations on the B3LYP optimized geometry, using extra polarization functions on P and H atoms, increase the computed

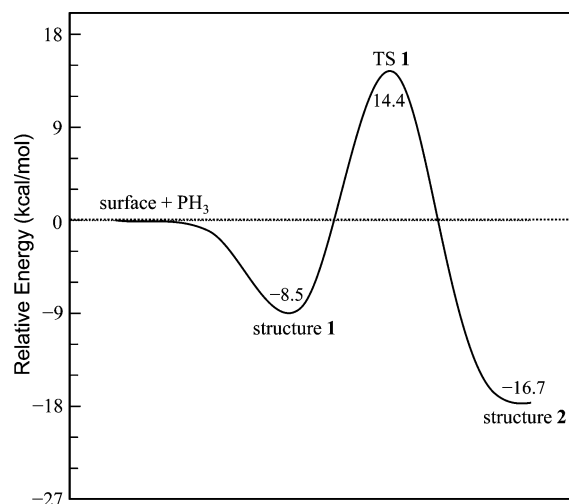


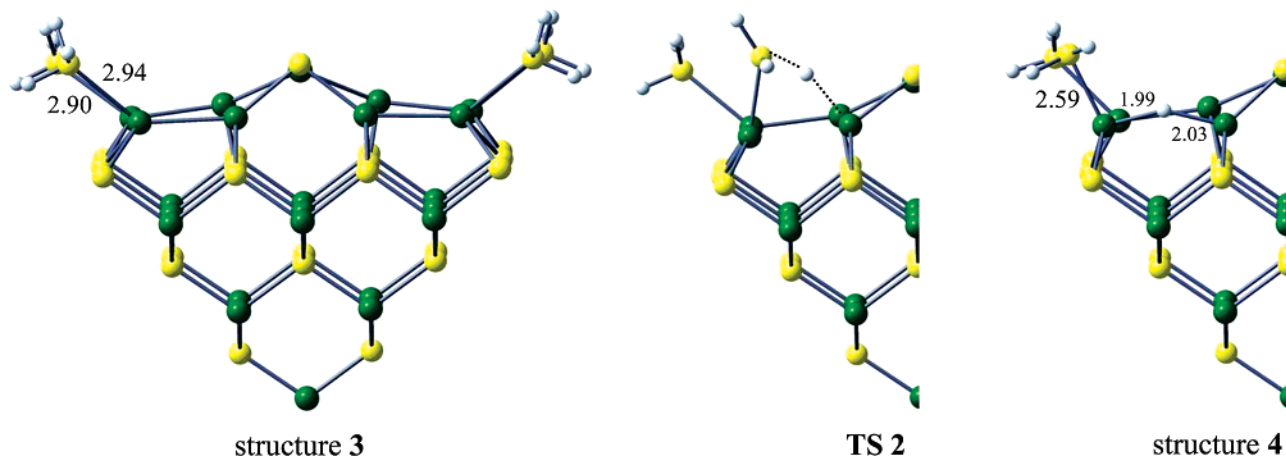
**Figure 3.** Potential energy diagram for phosphine adsorption and dissociation on the In–P mixed dimer.

binding energy by 2.5 kcal/mol. A table listing phosphine binding energies at different levels of theory can be found in the Supporting Information. In an earlier study,<sup>37</sup> Chaillet et al. also observed a change in PH<sub>3</sub> binding energy of approximately 3 kcal/mol when shifting from HF to MP2 calculations. These results clearly illustrate the importance of using post-SCF methods and larger basis sets in computing binding energy in such systems. We, therefore, suggest that the actual surface binding energies are, on average, 2–3 kcal/mol higher than those computed here.

The In–PH<sub>3</sub> dative bond length is 2.87 Å, consistent with previous ab initio studies on H<sub>3</sub>In–PH<sub>3</sub> that found In–P bond length to be 2.92 Å.<sup>37</sup> Binding of phosphine also causes significant changes in dimer buckling. Due to the more electron-rich environment now, the In atom moves up vertically, reducing the dimer tilt angle from 7.4° in the bare surface to 3° in structure **1**. Musgrave et al. observed a similar reduction in dimer tilting from 18° to 13° due to adduct formation on the silicon surface.<sup>38</sup>

(37) Chaillet, M.; Dargelos, A.; Marsden, C. J. *New J. Chem.* **1994**, *18*, 693.

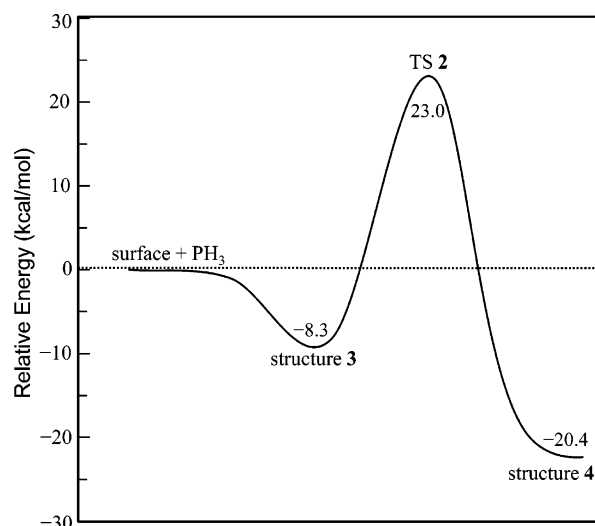
(38) Widjaja, Y.; Musgrave, C. B. *Surf. Sci.* **2000**, *469*, 9.



**Figure 4.** Phosphine adsorption on the In–In dimers. The structure on the left (**3**) shows dative bonded phosphines on all four surface dimers. The second (**TS2**) and the third (**4**) structures (partially truncated for clarity) represent phosphine dissociation on the phosphorus side of the mixed dimer. The distances are in Å.

Dissociation of  $\text{PH}_3$  leads to the migration of one H atom to the neighboring phosphorus center, and the remaining  $\text{PH}_2$  fragment now forms a covalent bond with the host In atom. This has been shown as structure **2** in Figure 2. The In–P mixed dimer length changes from 2.64 Å in **1** to 2.79 Å in **2**, as expected from its shift from covalent to significantly dative bonded nature. Also notable is a change in the direction of dimer tilting in this new structure. The vertical position of the In atom now makes the P atom down buckled, reversing the order found in either the bare surface or the dative bonded complex. The dissociated product is only 8.2 kcal/mol more stable than the dative bonded state. This relatively low stability of the dissociated species relative to the molecular complex is also observed on other compound semiconductor surfaces.<sup>20</sup> **TS1** in Figure 2 represents a transition structure that connects the two minima, **1** and **2**. Note that in **TS1**, the dimer tilt angle is almost zero, which justifies the intermediate nature of this state.  $\text{PH}_3$  decomposition is associated with a very high activation barrier, 11.9 kcal/mol above the entrance channel (23 kcal/mol above the complex **1**). A similar high barrier was also reported earlier for arsine adsorption on the GaAs surface.<sup>20</sup> The high barrier indicates a slow dissociation process, especially at room temperature. Note that in **2**, the lone pair on  $\text{PH}_2$  is projected away from the mixed dimer site. Similar orientations were also found for  $\text{NH}_2$  and  $\text{PH}_2$  groups on Si surfaces.<sup>11</sup>

**3.1.2.  $\text{PH}_3$  Adsorption on the In–In Dimers.**  $\text{PH}_3$  also binds to the surface In–In dimers. The associated binding energy is similar to that of the mixed dimer. However, all four indium dangling bonds in this layer are not equivalent. This is due to the nonequivalent local environments (symmetry breaking) created by the presence of the In–P mixed dimer on the top. Phosphine binding is slightly stronger (by 1.2 kcal/mol) on the In–In dimer at the cation site of the mixed dimer (refer to structure **3** in Figure 4). This side of the surface contains a chain of five indium atoms along the [110] direction. The long metallic chain stabilizes electron pairs donated by phosphine molecules more effectively compared to the other side where a phosphorus atom is sandwiched between two In–In dimers. This extra stability is also reflected in the corresponding dative bond lengths. The In– $\text{PH}_3$  distance is always shorter on the indium side of the adatom dimer (2.90 Å vs 2.94 Å). In addition, the stronger coordination makes lone pair electrons on the P atom to be less effective in screening the nuclear charge. This is reflected in shorter P–H bond lengths and higher symmetric stretching modes for phosphine molecules adsorbed on this side.

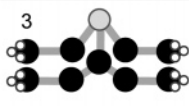
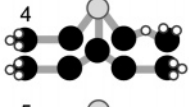
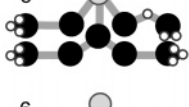
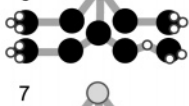
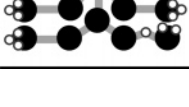


**Figure 5.** Potential energy diagram for adsorption and subsequent dissociation of phosphine (at the P-side of the mixed dimer) on the In–In dimers.

After phosphine dissociation, one of the hydrogen atoms migrates to the neighboring dimer site and inserts in between an In–In dimer bond to produce In–H–In, a three-center-two-electron bond. This new bonding state is shown as structure **4** in Figure 4. A similar bridged hydride structure was reported earlier for atomic H adsorption on the InP surface.<sup>39</sup> The bridged In–H<sub>b</sub> bond distances typically vary from 1.95 to 2.05 Å. Compared to the molecular complex (structure **3**), the dissociated product is 11–12 kcal/mol more stable when the  $\text{PH}_2$  group is positioned at the phosphorus side of the mixed dimer (structure **4**). A complete potential energy diagram for phosphine adsorption and subsequent dissociation on the metal dimer sites has been displayed in Figure 5. The kinetic barrier for the dissociation is 20.5 kcal/mol above the entrance level. We found a second conformational isomer for structure **4** based on a different spatial orientation of the  $\text{PH}_2$  group. This new conformer is listed as structure **5** in Table 1. **4**, in which the  $\text{PH}_2$  lone pair is facing a neighboring phosphine molecule, is slightly more stable (by 1 kcal/mol) than **5**. The additional stability comes from a weak

(39) Raghavachari, K.; Fu, Q.; Chen, G.; Li, L.; Li, C. H.; Law, D. C.; Hicks, R. F. *J. Am. Chem. Soc.* **2002**, *124*, 15119.

**Table 1. Different P–H Stretching Frequencies (cm<sup>-1</sup>) at the In–In Dimer Sites**

Structure	Mode	Theory	Expt.
	PH <sub>3</sub> <sup>s</sup>	2292	2285
	PH <sub>3</sub> <sup>as</sup>	2307	2301
		2328	2327
		2337	2339
	PH <sub>2</sub> <sup>s</sup>	2255	2262
	PH <sub>2</sub> <sup>as</sup>	2268	2262
	In–H–In	1111	a
	PH <sub>2</sub> <sup>s</sup>	2232	2226
	PH <sub>2</sub> <sup>as</sup>	2240	2242
	In–H–In	1124	a
	PH <sub>2</sub> <sup>s</sup>	2253	2262
	PH <sub>2</sub> <sup>as</sup>	2264	2262
	In–H–In	1228	a
	PH <sub>2</sub> <sup>s</sup>	2235	2226
	PH <sub>2</sub> <sup>as</sup>	2244	2242
	In–H–In	1235	a

<sup>a</sup> The experimental spectrum yields a broad band at this region (1150–1300 cm<sup>-1</sup>).

hydrogen-bonding interaction between the PH<sub>2</sub> and the PH<sub>3</sub> group on the neighboring dimers.<sup>40</sup>

On the other hand, phosphine decomposition at the In-side of the mixed dimer (structures **6** and **7** in Table 1) is less favorable both thermodynamically (by 3–4 kcal/mol) and kinetically (by 1–2 kcal/mol) due to the following reason. The distance between two neighboring In atoms on the unreconstructed InP(001) surface is 4.14 Å. This may be contrasted with the In–In dimer bond distance, which is computed to be 2.93 Å on the optimized cluster (Figure 1). Hydrogen insertion into the metal dimer bond expands the distance between two indium atoms to a value much closer to the surface lattice constant and, therefore, releases substantial amount of strain on the In–P back-bonds. This effect is more prominent at the P-side because of greater In–H–In bond distance. Note that, though the molecular complex is more stable on the In-side of the mixed dimer, the stability order is reversed in the dissociated species. Overall, the high activation barrier for product formation makes dissociation even less likely on the In–In dimers than on the In–P mixed dimer at 298 K. The possibility of simultaneous dissociation of all four phosphine molecules is thus unlikely at room temperature.

**3.2 Vibrational Analysis.** *3.2.1. Dative Bonded PH<sub>3</sub>.* The vibrational spectra for gas-phase phosphine (C<sub>3v</sub>) shows one mode with A<sub>1</sub> character at 2321 cm<sup>-1</sup> and a doubly degenerate mode with E character at 2326 cm<sup>-1</sup>.<sup>41</sup> In surface-adsorbed PH<sub>3</sub>, however, the overall point group symmetry is reduced to C<sub>s</sub>. This removes the degeneracy of the E mode, so that three vibrational lines are predicted. PH<sub>3</sub> in structure **1** exhibits a symmetric stretching mode at 2319 cm<sup>-1</sup> with relatively high intensity. Two asymmetric modes of low intensities, split only slightly, are computed at 2337 and 2340 cm<sup>-1</sup>. These frequencies are listed in Table 2. The absolute frequencies and the splitting between the symmetric and asymmetric modes, have both changed from gas phase to surface adsorbed species. We explain these

(40) Queeney, K. T.; Chabal, Y. J.; Raghavachari, K. *Phys. Rev. Lett.* **2001**, *86*, 1046.

(41) Tarrago, G.; Lacombe, N.; Levy, A.; Guelachvili, G.; Bezdard, B.; Drossart, P. *J. Mol. Spectrosc.* **1992**, *154*, 30.

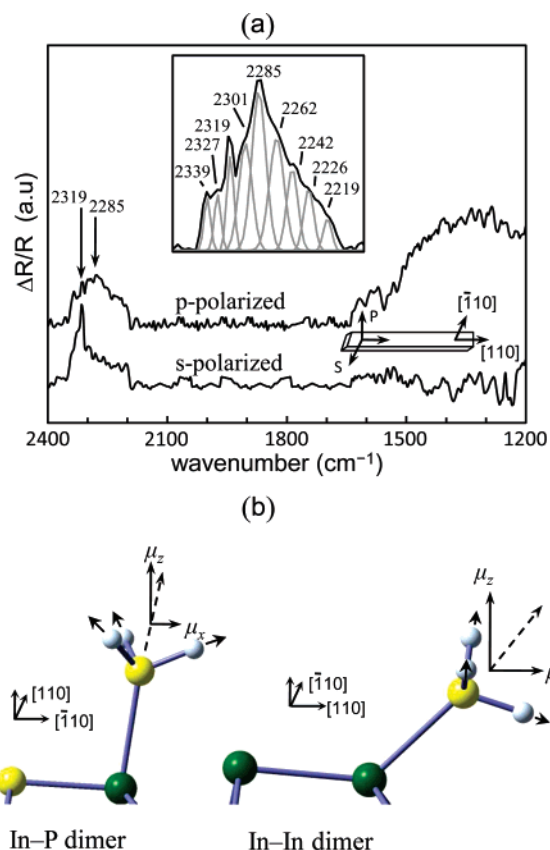


**Figure 6.** (a) Experimentally recorded surface IR spectra after phosphine adsorption at room temperature (using polarized lights). (Inset) P–H stretch region of the corresponding unpolarized IR spectrum. (b) The dipole derivative vectors for symmetric stretching of phosphine on In–P (left) and In–In dimers (right).

**Table 2. Different P–H Stretching Frequencies (cm<sup>-1</sup>) at the In–P Mixed Dimer Site**

Structure	Mode	Theory	Expt.
	PH <sub>3</sub> <sup>s</sup>	2319	2319
	PH <sub>3</sub> <sup>as</sup>	2339	2339
	PH <sub>2</sub> <sup>s</sup>	2238	2226
	PH <sub>2</sub> <sup>as</sup>	2247	2242
	PH	2279	—

changes as resulting from the substantial difference in the local dielectric environment. These computed frequencies and their intensities show excellent agreement with the experimental peaks positioned at 2319 and 2339 cm<sup>-1</sup>, respectively (inset, Figure 6a).

On the In–In dimers, we have considered the addition of one, two, and four phosphine molecules at a time to study partial and fully saturated surface dangling bonds. The symmetric stretch, when only one PH<sub>3</sub> molecule is present, appears at 2312 cm<sup>-1</sup>. This mode does not account for any of the spectral features in the experimental IR spectra. Surprisingly, the presence of one more PH<sub>3</sub> group on the neighboring dimer brings this mode down by 15 cm<sup>-1</sup>. This prompted us to saturate all four dangling bonds on the surface to monitor the case of complete surface coverage (structure **3**). Under these conditions, we find that the position of the symmetric mode ultimately drops down to 2292 cm<sup>-1</sup> (at the P-side), and the intensity associated with this mode

appears to be very high. We assign this mode as the one seen at  $2285\text{ cm}^{-1}$  in the experiment. An analogous symmetric  $\text{PH}_3$  stretching mode on the In-side of the mixed dimer appears at  $2307\text{ cm}^{-1}$ . Like the previous mode, this one also has relatively high intensity and is close to the experimental band seen at  $2301\text{ cm}^{-1}$ . We, therefore, suggest that, as soon as phosphine is exposed to the surface, it saturates all the surface dangling bonds. The intermediate surface structures containing one or two phosphine molecules have very minor or almost no contribution toward the observed IR spectra. This prediction is also supported by the observation that the spectral pattern does not change significantly at different phosphine dosages.<sup>25</sup> The asymmetric stretches corresponding to the two symmetric modes stated above are computed at  $2329$  and  $2337\text{ cm}^{-1}$ , respectively, both of them having very weak intensities. These two modes show good agreement with two weak bands observed at  $2329$  and  $2339\text{ cm}^{-1}$ , respectively.

We will now support the above spectral assignments based on the fact that the dipole moment derivative with respect to nuclear displacements along a normal mode is related to the intensity of IR absorption. For this, we refer to Figure 6a that shows that the peak at  $2319\text{ cm}^{-1}$  is equally s- and p-polarized when light travels along the [110] direction. Recall that this is also the direction of the In–In dimer bonds and perpendicular to the In–P adatom dimer bond. We have assigned this particular frequency coming from the symmetric stretching of  $\text{PH}_3$  molecule on the In–P adatom dimer. In this situation, the directions of the two dipole derivative vectors,  $\mu_x$  and  $\mu_z$ , are parallel to the direction of s- and p-polarized light, respectively (left part of Figure 6b), and hence, this mode responds to both polarizations. On the other hand, the band at  $2285\text{ cm}^{-1}$  almost disappears when an s-polarized light is used. Our calculations suggest that this band is produced by the symmetric P–H stretching of the phosphine molecules adsorbed on the In–In dimer sites. As shown in the right-hand side of Figure 6b, the net dipole moment derivative produced by the corresponding mode has components  $\mu_y$  and  $\mu_z$  which only respond to a p-polarized light. This explains the absence of any band at this position when an s-polarized light is used.

The splitting between the symmetric and asymmetric PH stretching modes in phosphine on the In–P adatom dimer is  $20\text{ cm}^{-1}$ . However, in case of the In–In dimers, the splitting between the two modes increases to  $40\text{ cm}^{-1}$ . It would be interesting in this context to look at this difference on other semiconductor surfaces. Hamers et al. reported a splitting of approximately  $20\text{ cm}^{-1}$  for dative bonded phosphine on the silicon surface.<sup>6</sup> However, the phosphine frequencies on this surface are a little lower ( $2270$  and  $2290\text{ cm}^{-1}$ , respectively) than on the indium phosphide surface. This may be due to the difference in the electronic nature of these two surfaces, the Si surface being more electron rich.

**3.2.2. After  $\text{PH}_3$  Dissociation.** The isolated P–H bond in structure **2** exhibits a single stretching mode at  $2279\text{ cm}^{-1}$ . No distinct peak is clearly visible at this position in the deconvoluted infrared spectra. However, it is possible that this peak is buried under the nearby very intense band at  $2285\text{ cm}^{-1}$ . The mixed dimer length in the dissociated product is  $2.79\text{ \AA}$ , a value somewhere in between In–P covalent ( $2.59\text{ \AA}$ ) and dative bond ( $2.89\text{ \AA}$ ) distance. Previously, for hydrogen adsorption on the P-rich InP surface, it was found that a four-fold coordinated P atom exhibits an isolated P–H stretch at  $2301\text{ cm}^{-1}$ , while a three-fold coordinated P atom with a lone pair on it produces the same mode at  $2225\text{ cm}^{-1}$ .<sup>36,42</sup> Therefore, the single P–H stretch

at  $2279\text{ cm}^{-1}$  in the dissociated species is consistent with the intermediate bonding state of its phosphorus atom.

Now we discuss vibrations of the phosphorus dihydrogen species present on the surface. All of them exhibit symmetric and asymmetric stretching modes that are separated by approximately  $10\text{ cm}^{-1}$ . However, the absolute frequencies associated with these modes depend on the position and spatial orientation of the individual  $\text{PH}_2$  units. In this context, one can notice that the  $\text{PH}_2$  groups in structures **2**, **5**, and **7** are almost geometrically equivalent. For example, the  $\text{PH}_2$  group in **2** exhibits symmetric and asymmetric vibrations at  $2238$  and  $2247\text{ cm}^{-1}$ . This may be compared to the corresponding modes in **5** and **7**. In structure **5**, these two modes appear at  $2232$  and  $2240\text{ cm}^{-1}$ , respectively. While in structure **7**, they appear at  $2235$  and  $2244\text{ cm}^{-1}$ , respectively. In the experimental IR spectra, we found one relatively broad band at  $2242\text{ cm}^{-1}$  and lower frequency peaks at  $2226\text{ cm}^{-1}$  and  $2219\text{ cm}^{-1}$ . We assign these three peaks as resulting from symmetric and asymmetric vibrations of the  $\text{PH}_2$  groups, described in structures **2**, **5**, and **7**. We note that the assignment of the two lower-frequency modes is tentative since the agreement between experiment and theory is only moderate in these cases and due to their relatively low intensities in the experiments.

On the other hand, the  $\text{PH}_2$  groups in structures **4** and **6** exhibit a different set of vibrations. As we mentioned earlier, they are involved in some kind of interdimer hydrogen bond formation. As a result, the corresponding stretching modes are blue-shifted by approximately  $20\text{--}25\text{ cm}^{-1}$ . For example, the symmetric and asymmetric vibrations in **4** appear at  $2255$  and  $2268\text{ cm}^{-1}$ . These modes are the origin of the band observed at  $2262\text{ cm}^{-1}$  in the experimentally recorded spectra. The vibrations of  $\text{PH}_3$  molecules in **4–7** do not produce any additional distinct modes. Overall, we see that the higher frequencies ( $>2280\text{ cm}^{-1}$ ) are in general produced by phosphine molecules dative bonded to the surface. On the other hand, the  $\text{PH}_2$  groups are responsible for bands seen in between  $2220\text{--}2260\text{ cm}^{-1}$ . In the latter case, the lone pair associated with the P atom effectively screens the nucleus from the hydrogen. This effect is reflected in higher P–H bond lengths (in  $\text{PH}_2$ ) and lower frequencies.

Finally, we focus on the stretching vibrations of the bridged metal hydrides produced by phosphine dissociation on the metal–metal dimer sites. We already know that In–H–In distances in structures **4** and **5** are on average  $0.1\text{ \AA}$  greater than in structures **6** and **7** (*vide supra*). This difference is also reflected in the corresponding stretching vibrations. For example, this particular mode in **4** (and **5**) is predicted to appear at  $1111\text{ cm}^{-1}$  (and  $1124\text{ cm}^{-1}$ ), while it is shifted upward by approximately  $120\text{ cm}^{-1}$  in **6** (and **7**). The theoretical results are consistent with the experimental spectrum that shows presence of a broad band at this region. However, due to the low resolution of this spectral region, it is not possible to quantitatively assign individual In–H–In stretching modes. In addition, we see that on the InP(100) surface, the  $\text{PH}_2$  groups can be oriented in a variety of different ways. These alternate configurations will lead to a variation in the In–H–In bond distances which explains the broadness of this band. Also note that bridged hydride stretches are seen only when a p-polarized light is used. This is easily understood since these In–H–In bonds are all parallel to the [110] axis and during vibrations, their dipole moments change only along this particular axis.

In a previous study, using a cluster unit approximately half of the size of the model adopted here, Raghavachari et al. computed frequencies around  $1350\text{--}1400\text{ cm}^{-1}$  for the In–H–In stretching (ref 39). In the current study, we find two

(42) Chen, G.; Cheng, S. F.; Tobin, D. J.; Li, L.; Raghavachari, K.; Hicks, R. F. *Phys. Rev. B* **2003**, *68*.

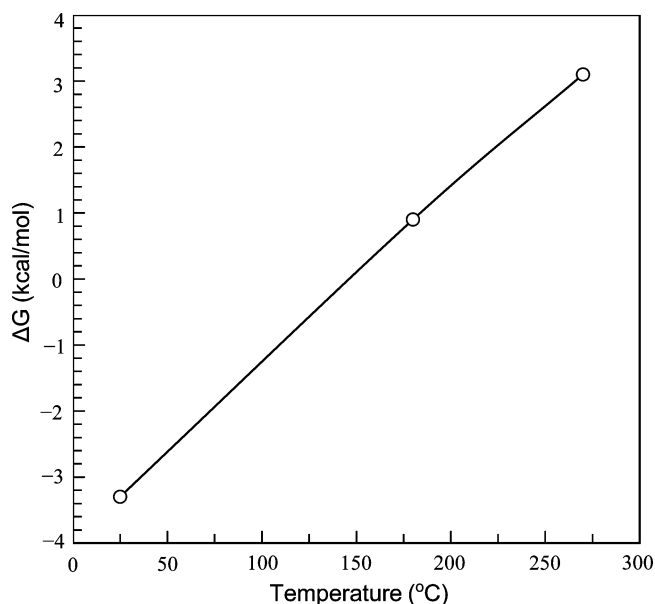
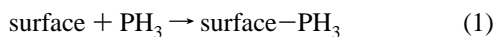


Figure 7. Plot of  $\Delta G$  as a function of temperature.

differences from the earlier results. First, the absolute frequency is shifted down by approximately  $100\text{ cm}^{-1}$ . In addition, we see a larger splitting of  $120\text{ cm}^{-1}$  when the position of the In–H–In group is shifted from anion to the cation side of the mixed dimer (4 and 5 vs 6 and 7). To determine the impact of the adatom dimer on these vibrations, we completely removed the In–P dimer from the top and recalculated the In–H–In stretching mode which appeared at  $1423\text{ cm}^{-1}$ . This suggests that the strain due to the presence of the In–P dimer brings down this particular stretching frequency significantly. Additionally, to verify the splitting, we replaced the In–P dimer, first with a P–P and then with an In–In dimer at the top and observed a difference of  $\sim 150\text{ cm}^{-1}$  in the In–H–In stretching frequencies in these two cases. These are much larger than the splitting of about  $40\text{ cm}^{-1}$  seen in the previous study. Hence, we conclude that the difference seen in the previous study results from using a truncated cluster model that yields somewhat different frequencies.

**3.3. Effect of Temperature.** The temperature-dependent infrared spectra in reference 25 show that the bands at  $2285$  and  $2319\text{ cm}^{-1}$ , arising from molecularly adsorbed PH<sub>3</sub> molecules, completely disappear at  $453\text{ K}$ . This indicates total absence of dative bonded structures at this higher temperature. To understand this process, we have computed the Gibbs free energy change ( $\Delta G$ ) for the initial complex formation at three different temperatures.



$$\Delta G = \Delta H - T\Delta S \quad (2)$$

These results are presented in Figure 7. At room temperature,  $\Delta G$  is negative and favors the process of surface dative bond formation. However, the dative bonded state becomes increasingly unfavorable at higher temperatures since  $\Delta G$  becomes more and more positive. For example, we compute the  $\Delta G$  value to be  $-3.3\text{ kcal/mol}$  at  $298\text{ K}$ , but it becomes  $0.9\text{ kcal/mol}$  and  $3.1\text{ kcal/mol}$  at  $453$  and  $543\text{ K}$ , respectively. The computed thermochemical parameters very well support the temperature dependence of the experimental IR spectra. While our computed binding energies of the complexes are low, dative bonded complexes with similarly small values of binding energy have been implicated on other semiconductor surfaces.<sup>3,20</sup>

The high barrier for phosphine dissociation makes the number of phosphine molecules traversing this barrier to be significantly low at room temperature. On the other hand, the same process is accompanied by a strong thermodynamic driving force which favors the dissociated species. Considering the presence of both such factors, it is expected that there will be some population of the PH<sub>2</sub> species even at  $300\text{ K}$ .

#### 4. Conclusions

In conclusion, we present here the initial atomic structure of indium phosphide surfaces after phosphine exposure at room temperature. The surface empty dangling bonds are completely saturated, forming dative bonds with the precursor molecules. Despite its low bond strength, it is possible to trap this dative bonded state at room temperature because of the high kinetic barrier for phosphine dissociation and the relatively low additional stability of the dissociated products. Partial dissociation of phosphine is still possible at room temperature as evidenced from the presence of infrared modes associated with the PH and PH<sub>2</sub> species. However, the equilibrium is mostly shifted toward the dative bonded state. The assignment of three of the most intense peaks observed at  $2285$ ,  $2301$ , and  $2319\text{ cm}^{-1}$ , all originating from symmetric stretches of molecularly adsorbed phosphines, is consistent with this picture. Our observation is unprecedented since the dative bonded state of PH<sub>3</sub> is known to completely dissociate on Si and GaAs surfaces well below the room temperature. This work is also an important starting point toward establishing the complete mechanism of converting an In-rich surface into a P-rich domain by phosphine adsorption.

**Acknowledgment.** We acknowledge financial support of this work in the form of grants from the Petroleum Research Fund (Grant No. PRF 43465-AC10) and from the NSF (Grant No. CHE-0616737) at Indiana University.

**Supporting Information Available:** Binding energies of phosphine in InH<sub>3</sub>–PH<sub>3</sub> computed at different levels of theory have been listed in Table S1. This material is available free of charge via the Internet at <http://pubs.acs.org>.

LA700790H